RESEARCH PAPER

MpmiR319 promotes gemma/gemma cup formation in the liverwort *Marchantia polymorpha*

Authors: Kazutaka Futagami[1], Masayuki Tsuzuki[1,2 *], Yuichiro Watanabe[1 *]

[1] Department of Life Sciences, Graduate School of Arts and Sciences, The University of Tokyo, Tokyo 153-8902, Japan

[2] Faculty of Agriculture and Marine Sciences, Graduate School of Integrated Arts and Sciences, Kochi University, Nankoku, Kochi 783-8502, Japan

* Corresponding authors

E-mail: ft.kz.m9m@gmail.com (K. Futagami)

mtsuzuki@kochi-u.ac.jp (M. Tsuzuki)

cyuiwat@g.ecc.u-tokyo.ac.jp (Y. Watanabe)

Highlight

This study demonstrates Mp*miR319* expression affects gemma cup and gemma formation during *Marchantia polymorpha* vegetative propagation by suppressing its target mRNAs.

ORCID

Kazutaka Futagami: https://orcid.org/0000-0002-3321-6508

Masayuki Tsuzuki: https://orcid.org/0000-0002-0642-1143

Yuichiro Watanabe: https://orcid.org/0000-0002-7139-4903

Abstract

After microRNAs (miRNAs) were initially detected as approximately 21-nt sequences in plants, miRNA-mediated regulation of target gene expression was characterized in many cases. The sequences of miR159/319 family miRNAs are highly conserved and their development-related roles have been comprehensively characterized in dicot and monocot plants. However, their effects in basal land plants remain relatively unknown. We used a CRISPR/Cas9 system to edit genome sequences at Mp*MIR319a* and/or Mp*MIR319b* loci. Mutant *mir319b* lines developed relatively few gemma cups, while mutant *mir319a* lines produced relatively few gemmae in each gemma cup. Earlier 5′-RACE or degradome analyses suggested that Mp*miR319* targets Mp*RKD* and Mp*R2R3-MYB21* transcripts and suppresses expression. To determine whether these candidate genes influence the *mir319a/mir319b* phenotype we constructed miR319-resistant Mp*RKD* (mMp*RKD*) and Mp*R2R3-MYB21* (mMp*R2R3-MYB21*) by decreasing the complementarity to miR319. We also introduced the genes into wild-type liverwort and screened for phenotypic changes. We observed that mMp*RKD* resulted in gemma/gemma cup-less liverwort mutants, but mMp*R2R3-MYB21* did not. No major adverse effects were detected during male and female reproductive development induced by far-red illumination. These results indicate that miR319 influences gemma formation mainly by repressing Mp*RKD* expression rather than Mp*R2R3-MYB21* expression.

Keywords: liverwort, *Marchantia polymorpha*, gemma, gemma cup, notch, microRNA, RKD transcription factor, R2R3MYB transcription factor

45 ***Introduction***

46 The complementarity to their target mRNA sequences is generally greater for plant
47 microRNAs (miRNAs) than for animal miRNAs (Rhoades et al., 2002)(Lin and Bowman,
48 2018). Each plant miRNA can target a limited number of mRNAs. Accordingly, mRNA(s)
49 targeted by each miRNA can be predicted by searching genome sequence data for a
50 sequence complementary to the miRNA sequence of interest. Recent studies revealed that
51 land plants have 300–500 lineage-specific diverse miRNAs (Axtell et al., 2007)(Lin and
52 Bowman, 2018)(Pietrykowska et al., 2022). Earlier *in vivo* studies on miRNAs conserved
53 among land plants showed that their target mRNAs are transcribed from highly conserved
54 cognate genes across phyla (Axtell et al., 2007)(Tsuzuki et al., 2019)(Alaba et al.,
55 2015)(Pietrykowska et al., 2022). Such conserved miRNA–target mRNA modules may
56 form a core set of functionally and biologically important gene regulatory circuits in land
57 plants. Moreover, as few as seven miRNA families are highly conserved from the
58 liverwort *Marchantia polymorpha* and the moss *Physcomitrella patens* to angiosperms
59 (Axtell et al., 2007)(Tsuzuki et al., 2016)(Lin et al., 2016b)(Pietrykowska et al., 2022).
60 However, most liverwort miRNAs have not been studied sufficiently to determine how
61 common or specific they are among land plants. Additional experimental data are needed
62 to substantiate the biological significance of highly conserved miRNAs in basal land
63 plants. Among conserved miRNAs, miR159/319 family members are unique because
64 their target mRNA species may have changed during phylogenetic diversification
65 (Palatnik et al., 2007). In Arabidopsis, miR319 preferentially targets mRNAs of
66 *TEOSINTE BRANCHED1*, *CYCLOIDEA*, and *PROLIFERATING CELL FACTOR* genes

67 (Martín-Trillo and Cubas, 2010)(Kosugi and Ohashi, 1997). These genes encode basic-
68 helix-loop-helix transcription factors that redundantly affect cotyledon boundary
69 specification and leaf serration (Palatnik et al., 2003)(Koyama et al., 2017).
70 *Marchantia polymorpha* is a liverwort that is a valuable emerging model species used
71 in studies on land plant diversification, which have generated increasing amounts of
72 information and resources for comparative evolution research (Bowman et al., 2017). In
73 *M. polymorpha*, Mp*miR319* targets mRNAs of *MpR2R3-MYB21* (Arabidopsis MYB33-
74 like transcription factor belonging to the GAMYB family) (Lin et al., 2016b)(Tsuzuki et
75 al., 2016) and RWP-RK DOMAIN (RKD)-containing transcription factor genes (Lin et
76 al., 2016b) according to a 5′-RACE or degradome analysis. Thus, Mp*miR319* may have
77 some regulatory effects on such candidate target genes, but this possibility remains to be
78 experimentally verified.
79
80 ***Materials and methods***
81 **Plant materials and growth conditions**
82 Takaragaike-1 (Tak-1, male) and Takaragaike-2 (Tak-2, female) were used as wild-type
83 *M. polymorpha* samples (Ishizaki et al., 2008). Plants were grown asexually on half-
84 strength Gamborg's B5 medium (FUJIFILM Wako Pure Chemical Co., Osaka, Japan)
85 (Gamborg et al., 1968) containing 0.5 g/l 2-morpholinoethanesulfonic acid (MES, Tokyo
86 Chemical industry Co., Tokyo) and 1% (w/v) agar (STAR Agar L-grade, RIKAKEN,
87 Tokyo) under continuous white fluorescent light at 22 °C. To induce the sexual
88 reproductive phase, plants were grown at 22 °C under continuous light conditions

89 provided by a mixture of white fluorescent light and far-red (FR) light-emitting diodes
90 (OSXXXXT3C1E, OptoSupply, Hong Kong; peak emission at 730 nm, with a full width
91 at half-maximum of 20 nm).
92
93 **Transformation and mutant selection**
94 Regenerating thalli (for *mir319a* or *mir319b* mutants) (Kubota et al., 2013) and a G-
95 AgarTrap method (to generate gMp*RKD*, mMp*RKD*, gMp*MYB21*, and mMp*MYB21*
96 lines) (Tsuboyama and Kodama, 2018) were used to transform *M. polymorpha*. Briefly,
97 transformed plants were selected on half-strength Gamborg's B5 medium containing 0.5
98 g/l MES, 1% (w/v) agar, 100 μg/ml cefotaxime and 10 μg/ml hygromycin (for
99 pMpGWB101 and pMpGE010), or 100 μg/ml cefotaxime and 0.5 μM chlorsulfuron (for
100 pMpGWB301 and pMpGE011). After screening T_1 plants on drug-supplemented media,
101 we obtained approximately 10 candidate lines for each guide RNA (gRNA) in the male
102 and female genetic backgrounds.
103
104 **Genomic DNA extraction**
105 Genomic DNA was extracted from Tak-1 thalli using the DNeasy Plant Mini kit (Qiagen,
106 Hilden, Germany) according to the manufacturer's recommendations.
107
108 **Plasmid construction for the CRISPR/Cas9 system**
109 We employed the CasFinder Tool (https://marchantia.info/tools/casfinder/) to design
110 gRNAs to target Mp*miR319a* and/or Mp*miR319b* loci. The pMpGE_En03 vector

111 (Sugano et al., 2018) was used to clone oligonucleotide pairs to express gRNAs:
112 pMpGE_En03-gRNA1, pMpGE_En03-gRNA3, and pMpGE_En03-gRNA4.
113 pMpGE010 and pMpGE011 were used for Cas9 expression (Sugano et al., 2018).
114 The *mir319a*^{ge}, *mir319b*^{ge}, and *mir319ab*^{ge} mutants were selected as described
115 previously (Tsuzuki et al., 2019). Using genomic DNA as the template, *MIR319A* and
116 *MIR319B* sequences were amplified by PCR using PrimeSTAR HS DNA polymerase
117 (TaKaRa Bio, Kusatsu, Japan) and the primer pairs MpMIR319aF1 and MpMIR319a-R1
118 or MpMIR319bF2 and MpMIR319b-R2. Amplified products were sequenced according
119 to the Sanger method. Details regarding the PCR and genomic sequencing primers are
120 listed in Table S1. Mp*MIR319A* and Mp*MIR319B* genomic sequences in *mir319a*^{ge},
121 *mir319b*^{ge}, and *mir319ab*^{ge} mutant plants (T_1 generation) are provided in Figure 1.
122

123 **Construction of miR319-resistant Mp*RKD* and Mp*R2R3-MYB21* transgenes**

124 To obtain the wild-type *RKD* gene segment, the genomic sequence from the Mp*RKD*
125 promoter region (3,827 bp upstream of the translation initiation codon) to the 3′
126 untranslated region (UTR) (568 bp downstream of the translation termination codon) was
127 amplified by PCR using Tak-1 genomic DNA, PrimeSTAR HS DNA polymerase
128 (TaKaRa Bio), and primers IF-Hind-pRKD-F and Inf-gMpRKD-Sal-R. To create the
129 miR319-resistant Mp*RKD* gene segment, two PCR fragments were amplified using Tak-
130 1 genomic DNA as well as the IF-Hind-pRKD-F and mRWP_RK-R primer set and the
131 mRWP_RK-F and Inf-gMpRKD-Sal-R primer set to specifically mutate the miR319
132 target sequence in the Mp*RKD* 3′ UTR sequence. The In-Fusion Cloning kit (TaKaRa

133 Bio) was used to insert the PCR fragments into the pMpGWB300 vector that had been
134 cleaved by *Hin*dIII and *Sal*I to generate the pMpGWB300:proMpRKD:gMpRKD and
135 pMpGWB300:proMpRKD:mMpRKD recombinant plasmids.
136 To obtain the wild-type *MYB21* gene segment, the Mp*MYB21* promoter region (3008 bp
137 upstream of the translation initiation codon) to the initiation codon, was first amplified
138 by PCR using Tak-1 genomic DNA, PrimeSTAR HS DNA polymerase, and primers
139 Hind-pMpMYB21-3000-F and Sal-pMpMYB21-R, cloned into pMpGWB100 after
140 both being restricted with *Hin*dIII and *Sal*I to obtain pMpGWB100-pMYB21. Wild-type
141 *MYB21* gene segment (gMYB21) from halfway of promoter region to the termination
142 codon (4244 bp) were amplified using Tak-1 genomic DNA and primers pMYB33-
143 459F and Bam-MpMYB33-R2. To create the miR319-resistant Mp*MYB21* gene segment,
144 two PCR fragments were amplified using gMYB21 fragment as well as the pMYB33-
145 459F and mMYB33-R set and the mMYB33-F and Bam-MpMYB33-R2 primer
146 set to specifically mutate the miR319 target sequence in the Mp*MYB21*
147 coding sequence. The obtained PCR fragments were mixed and subjected to
148 the next PCR reaction using primers pMYB33-459F and Bam-MpMYB33-R2
149 to obtain miR319 resistant MYB21 gene body fragment (mMYB21). The gMYB21 and
150 mMYB21 fragments were cloned separately into the pMpGWB100 vector, after being
151 compatibly restricted with *Nru*I and *Bam*HI, to generate the pMpGWB100:pgMp*MYB21*
152 and pMpGWB100:pmMp*MYB21*.
153 *M. polymorpha* was transformed with the recombinant plasmids as described previously
154 (Tsuboyama et al., 2018a)(Tsuboyama and Kodama, 2018).

155

156 ***Results***

157 **Guide RNA-mediated editing of *MIR319* genes**

158 A previous study revealed *M. polymorpha* has a relatively simple genome because of
159 limited gene redundancy (Bowman et al., 2017). *M. polymorpha* has two *MIR319* coding
160 loci, both of which produce an identical mature miRNA sequence (5′-
161 $_{p}$CUUGGACUGAAGGGAGCUCCC$_{OH}$-3′) (Lin et al., 2016b; Tsuzuki et al., 2016). The
162 two *MIR319* loci have been annotated (*M. polymorpha* genome ver.6.1) as Mp*MIR319A*
163 (Mp3g08965) and Mp*MIR319B* (Mp4g01845) (Fig. 1A).

164 We focused on whether Mp*MIR319a* and/or Mp*MIR319b* loci are functional. To analyze
165 the possible biological functions of miR319 in *M. polymorpha*, we edited two annotated
166 Mp*miR319* coding sequences to obtain mutants, which were examined for phenotypic
167 changes. Specifically, we designed gRNA#1 for *MIR319A* (Fig. 1B) and gRNA#3 and #4
168 for *MIR319B* (Fig. 1C) and constructed vectors to introduce indel mutations at the
169 respective *MIR319* loci using a CRISPR/Cas9 genome-editing system (Sugano et al.,
170 2014)(Sugano et al., 2018). We adopted an *Agrobacterium*-mediated transformation
171 protocol to introduce the vectors into Tak-1 thalli to express the gRNAs and Cas9 (Sugano
172 et al., 2014)(Tsuboyama et al., 2018b). After the drug-based selection of G_1 plants, we
173 amplified the targeted genomic sequences from selected G_1 thalli and analyzed the PCR
174 products via Sanger sequencing to confirm indel mutations were present at the target loci.
175 Multiple lines with indel mutations at the Mp*MIR319a* or Mp*MIR319b* locus were
176 generated. Several representative lines with similar phenotypes were selected (Fig. 1B

177 and C) for the subsequent analysis. The selected mutants with indel mutations at the
178 Mp*mir319a* locus were designated as *mir319a*$^{ge-1}$ *a* #5 and *mir319a*$^{ge-1}$ *a* #10, whereas
179 the selected mutants with indel mutations at the Mp*mir319b* locus were designated as
180 *mir319b*$^{ge-3}$ *b* #11, *mir319b*$^{ge-3}$ *b* #15, *mir319b*$^{ge-4}$ *b* #6, and *mir319b*$^{ge-4}$ *b* #9.
181

182 ***miR319a* and *miR319b* mutant thalli exhibited abnormal gemma cup production**

183 Although the *mir319a*^{ge} and *mir319b*^{ge} mutant plants grew as fast as the wild-type Tak-1
184 plants, they produced gemma cups less frequently than Tak-1 plants (Fig. 2). More
185 specifically, compared with wild-type Tak-1 plants, significantly fewer *mir319a*$^{ge-1}$ (*a* #5
186 and *a* #10) and *mir319b*$^{ge-3}$ (*b* #11 and *b* #15) plants produced gemma cups
187 (approximately half as many). Gemma cup production was most inhibited in the
188 *mir319b*$^{ge-4}$ (*b* #6 and *b* #9) plants. We speculated that both *mir319a* and *miR319b* alleles
189 somehow affect gemma cup formation during dorsal organ formation in thalli. In addition,
190 *mir319a*$^{ge-1}$ (*a* #5 and *a*#10) mutants produced fewer gemmae in each gemma cup than
191 the wild-type plants (Fig. 3), whereas the *mir319b*$^{ge-3}$ (*b* #11 and *b* #15) mutants and the
192 wild-type plants did not differ in terms of the number of gemmae in each gemma cup (Fig.
193 3). These observations suggest that miR319 contributes to the formation of gemmae and
194 gemma cups in *M. polymorpha* by regulating target gene expression.
195 We also created similar *mir319a*^{ge} and *mir319b*^{ge} mutants using female Tak-2 plants. A
196 decrease in gemma cup formation was also detected in the Tak-2-based mutants (data not
197 shown). Thus, we focused mainly on lines with a Tak-1 genetic background to study the
198 miR319 function during vegetative growth stages.

199

200

201 **Knockout of both *miR319a* and *miR319b* loci did not result in additive defects**

202 The *mir319a* and *mir319b* knockout lines exhibited similar phenotypic defects in terms
203 of the production of gemma cups/gemmae. We analyzed whether the two loci additively
204 affect liverwort vegetative organ formation by creating and characterizing double
205 knockout mutants. We were unable to obtain a double mutant via a single transformation
206 involving two vectors. Thus, we targeted the *MIR319a* locus of *mir319b*$^{ge\text{-}3}$ *b* #15 with
207 pMpGE_En03-gRNA1. After several trials, we obtained a double knockout line that had
208 a 5-base deletion in the *MIR319a* locus identical to *mir319a*$^{ge\text{-}1}$ *a* #10 in addition to a 1-
209 base addition in the *MIR319b* locus (Fig. 1D). For brevity, the mutant line was named
210 *miR319ab #10/15* (Fig. 1D). In terms of the number of developed gemma cups and
211 gemmae, the *miR319ab #10/15* mutant phenotype did not differ from the *miR319a* and
212 *mir319b* mutant phenotypes (Fig. 2, *ab* #10/15).

213

214 **Regulation of Mp*RKD* by miR319 influences gemma cup formation**

215 An earlier degradome analysis indicated that Mp*RKD* (formerly *RWP-RK DOMAIN-*
216 *CONTAINING 1*) and Mp*MYB33* mRNAs are targeted by Mp*miR319* (Lin et al., 2016a).
217 In the current study, we assessed whether the susceptibility of either or both of these
218 mRNA genes to miR319 affects gemma/gemma cup formation. Mp*RKD* encodes an
219 RWP-RK domain-containing transcription factor that is an evolutionarily conserved
220 regulator of germ cell differentiation (Koi et al., 2016)(Rövekamp et al., 2016).

221 Additionally, it was reported that Mp*RKD* is expressed on gemma cup rims (Koi et al.,
222 2016) and is necessary for normal gemma cup growth (Rövekamp et al., 2016).
223 Accordingly, we examined whether downregulated Mp*RKD* expression due to miR319 is
224 linked to gemma/gemma cup formation. We constructed a mutated *RKD* coding sequence
225 that is unaffected by miR319.

226 The 21-nt sequence complementary to miR319 started from 4 nt downstream of the stop
227 codon in the *M. polymorpha RKD* (Mp*RKD*) mRNA sequence. We constructed a miR319-
228 resistant form of the Mp*RKD* gene (designated as mMp*RKD*; Fig. 4A) by introducing a
229 12-base substitution to decrease the complementarity to Mp*miR319*. The mMp*RKD* gene
230 was placed downstream of its own 3.8 kb promoter sequence in the pMpGWB300 vector
231 (Ishizaki et al., 2015). As a control, we cloned wild-type Mp*RKD* (designated as
232 gMp*RKD*) in the same vector. The mMp*RKD* gene produces *RKD* mRNA that is
233 insensitive to miR319, whereas gMp*RKD* mRNA is sensitive to miR319. The gMp*RKD*
234 and mMp*RKD* genes were introduced into separate Tak-1 wild-type plants to obtain
235 gMp*RKD* and mMp*RKD* lines. Both gMp*RKD* and mMp*RKD* plants had similar thallus
236 growth rates, but the mMp*RKD* plants failed to produce gemma cups (Fig. 5: mMpRKD).
237 The gemma cup-less phenotypes were similar to those of the *mir319a*$^{ge\text{-}1}$ or *miR319ab*
238 *#10/15* mutants (Fig. 5; mir319ab #10/15). In contrast, the gMp*RKD* lines produced
239 gemma cups similar to the wild-type Tak-1 control (Fig. 5; gMpRKD). Therefore, the
240 sequences complementary to Mp*miR319* in Mp*RKD* mRNA are critical for
241 gemma/gemma cup formation. Moreover, Mp*RKD* translation is likely suppressed by
242 Mp*miR319*.

243 As mentioned earlier, the miR319 target sequence is located in the 3′ UTR downstream
244 of the *RKD* termination codon sequence. Thus, we designed another miR319-insensitive
245 *RKD* gene (Mp*RKD*-Δ3′UTR) by removing the complementary sequences from the 3′
246 UTR without disturbing *RKD* translation (Fig. S1A). When we introduced Mp*RKD*-
247 Δ3′UTR into liverwort, thalli were able to grow, but only a few gemma cups developed,
248 similar to the mMp*RKD* liverwort (Fig. S1B).
249
250 **Gemma cup/gemma formation was unaffected by miR319-resistant Mp*MYB21***
251 According to a 5′-RACE or degradome analysis, Mp*MYB21* is also a potential target
252 gene of miR319 (Tsuzuki et al., 2016)(Lin et al., 2016b). To test whether the regulation
253 of *MYB21* expression by miR319 affects gemma cup formation, we created a miR319-
254 resistant Mp*MYB21* (mMp*R2R3-MYB21* or m*MYB21*) that was placed under the control
255 of its own promoter similar to the Mp*RKD* gene (Fig. 4B). mMp*R2R3-MYB21* was
256 introduced into wild-type Tak-1 liverwort. The obtained m*MYB21* liverwort lines
257 produced thalli with gemma cups/gemmae, but the thalli had shapes slightly different
258 from the wild-type thalli (Fig. 5; mMpR2R3-MYB21). These results indicate that
259 Mp*R2R3-MYB21* affects gemma cup/gemma formation substantially less than Mp*RKD*
260 (if at all).
261
262
263 **mMp*RKD* plants developed deformed antheridiophores/archegoniophores, but**
264 **normal sperm and eggs**

265 It was previously reported that Mp*RKD*, which is expressed in developing eggs and
266 sperm precursors, regulates egg and sperm formation in *M. polymorpha* (Koi et al.,
267 2016)(Rövekamp et al., 2016). Thus, we analyzed germ cell, gametangia, and
268 gametangiophore differentiation (Yamaoka et al., 2021)(Shimamura, 2016) in gMp*RKD*
269 and mMp*RKD* liverworts. In response to FR illumination, the mMp*RKD* line with the
270 Tak-1 genetic background developed male gametophytes (Fig. 6C) at nearly the same
271 time as the gMp*RKD* liverwort (Fig. 6A). In addition, mMp*RKD* antheridiophores had
272 almost normal stalked receptables, except for their irregular asymmetrical shape (Fig. 6C,
273 D). Antheridia formed and protruded outward, but they were not surrounded by
274 antheridiophores in mMp*RKD* lines (Fig. 6E, F). Sperm mobility was similar in the
275 mMp*RKD*, wild-type Tak-1, and gMp*RKD* liverworts.
276 We also introduced gMp*RKD* and mMp*RKD* genes into wild-type Tak-2 liverwort and
277 then checked whether archegonia/archegoniophore development was affected. We
278 generated transgenic lines using two constructs (Fig. 4A). Under FR light, the mMp*RKD*
279 liverwort in the Tak-2 genetic background developed female gametophytes as early as the
280 gMp*RKD* liverwort, but its archegoniophores (Fig. 6I) differed from those of gMp*RKD*
281 (Fig. 6G) or Tak-2 plants in terms of shape. mMp*RKD* archegoniophores had short digits
282 (Fig. 6I,J), but produced normal archegonia. Furthermore, in terms of their appearance,
283 the mMp*RKD* archegonia (Fig. 6K) were almost identical to the archegonia of gMp*RKD*
284 (Fig. 6H) or wild-type Tak-2 liverwort.
285
286

287 **Discussion**

288 When we profiled *M. polymorpha* miRNAs by small RNA-seq analysis, we tried to
289 overexpress miR319 precursor RNAs in wild-type liverwort to clarify their biological
290 functions. The ectopic expression of a miR319 precursor in liverwort adversely altered
291 the development of gemma cups (Tsuzuki et al., 2016). We speculated that the balanced
292 expression of miR319/target mRNAs is necessary for normal gemma cup development
293 in *M. polymorpha*. Our RACE assay detected the cleavage of Mp*MYB21* mRNA, which
294 encodes a homolog of Arabidopsis *MYB33*. An earlier RNA degradome analysis revealed
295 Mp*RKD* (formerly *RWP-RK DOMAIN-CONTAINING 1*) mRNA is also cleaved by
296 MpmiR319 (Lin et al., 2016b). Mp*RKD* was previously investigated using *Marchantia*
297 mutants (Koi et al., 2016)(Rövekamp et al., 2016). These studies showed that Mp*RKD* is
298 essential for normal germ cell differentiation in both male and female gametophytes, but
299 it is also involved in the differentiation of non-reproductive cells surrounding the
300 antheridia, developing egg, and sperm precursors (Koi et al., 2016)(Rövekamp et al.,
301 2016). Mp*RKD* also influences gemma cup formation (Rövekamp et al., 2016). This gene
302 is transcribed at the edge of gemma cups and the meristematic regions of apical notches
303 (Koi et al., 2016)(Rövekamp et al., 2016). It remains unknown whether miR319 organizes
304 gene regulatory networks with Mp*RKD* and further research will clarify.

305 The gemma cup formation has been histologically characterized. Founder gemmae
306 arise directly from above the center of the apical notch of the thallus, which is followed
307 by the formation of the cup rims surrounding gemmae (Shimamura, 2016). Our findings
308 combined with the available data suggest that Mp*RKD* is involved in various cell

309 proliferation stages, resulting in the formation of a variety of *M. polymorpha* tissues,
310 including gemmae/gemma cups. Nevertheless, additional research is needed to clarify
311 how gemma cups are organized by miR319-mediated gene regulatory networks.

312 There are several reports of mutants with defective pathways mediating gemma cup
313 formation in thalli, including the RopGEF KARAPPO (Hiwatashi et al., 2019), GCAM1
314 (Yasui et al., 2019), and MpKAI2–ligand signaling (Komatsu et al., 2023) pathways.
315 However, the pathway facilitating the formation of gemma cups from the apical notch has
316 not been fully determined. Solly *et al.* showed that growth rate heterogeneity determines
317 the flattened shape of *Marchantia* thalli and that the basic shapes are due to growth rate
318 differences specified by apical notch activities (Solly et al., 2017). Recently, Romani *et*
319 *al*. comprehensively revealed the activities of approximately 450 putative transcription
320 factor gene promoters by analyzing the respective reporter fusion constructs (Romani et
321 al., 2024). They generated a map of expression domains for each transcription factor gene
322 related to gemma growth and identified more than 100 promoters that are active
323 specifically in the apical notch. The mechanism underlying the formation of gemma cups
324 may be much more complex than expected.

325 The *mir319a* and *mir319b* loci differentially contribute to gemma cup formation,
326 possibly because of some differences in cell-specific transcription or processing
327 efficiency, but this possibility will need to be tested in future studies. In the moss *P. patens*,
328 miR159/319, which are encoded in the genome, may target mRNAs for cyclin domain
329 proteins and two MYB transcription factors (Axtell et al., 2007). Moreover, miR159/319
330 families are highly conserved from bryophytes to angiosperms, but their biological

functions might be more diverse than we initially imagined.

Supplementary Data

Table S1 Primers used in this study

Fig. S1 Introduction of miR319-insensitive *RKD* genes into wild-type liverwort resulted in the production of relatively few gemma cups.

Acknowledgements

We thank Kohchi, T. and Yamaoka, S. of Kyoto University, Ishizaki, K. of Kobe University, Shimamura, M. of Hiroshima University, and Nakajima, K. of NAIST for their advice and discussions. We also thank Bahari M. and Edanz (https://jp.edanz.com/ac) for editing a draft of this manuscript.

Author contributions

KF performed the experiments. KF and MT designed the experiments. KF, YW, and MT wrote the manuscript.

Conflict of interest

The authors declare that they have no competing financial interests related to this work.

Funding

This work was supported by MEXT KAKENHI (21K06225 and 24K09499 to Y.W.) and the Japan Society for the Promotion of Science funding for Bilateral Joint Research Projects FY2022-23 (JPJSBP 120224601 to Y.W.).

Data Availability

Relevant data can be found within the manuscript and its supplementary data online.

References

Alaba S, Piszczalka P, Pietrykowska H, Pacak AM, Sierocka I, Nuc PW, Singh K, Plewka P, Sulkowska A, Jarmolowski A, et al (2015) The liverwort Pellia endiviifolia shares microtranscriptomic traits that are common to green algae and land plants. New Phytol **206**: 352–367

Axtell MJ, Snyder JA, Bartel DP (2007) Common functions for diverse small RNAs of land plants. Plant Cell **19**: 1750–1769

Bowman JLJL, Kohchi T, Yamato KT, Jenkins J, Shu S, Ishizaki K, Yamaoka S, Nishihama R, Nakamura Y, Berger F, et al (2017) Insights into Land Plant Evolution Garnered from the Marchantia polymorpha Genome. Cell **171**: 287-304.e15

Gamborg OL, Miller RA, Ojima K (1968) Nutrient requirements of suspension cultures of soybean root cells. Exp Cell Res **50**: 151–158

Hiwatashi T, Quan KL, Yasui Y, Takami H, Kajikawa M, Kirita H, Sato M, Wakazaki M, Yamaguchi K, Shigenobu S, et al (2019) The RopGEF KARAPPO Is Essential for the Initiation of Vegetative Reproduction in Marchantia polymorpha. Curr Biol **29**: 3525-

375 3531.e7

376 **Ishizaki K, Chiyoda S, Yamato KT, Kohchi T** (2008) Agrobacterium-mediated transformation
377 of the haploid liverwort Marchantia polymorpha L., an emerging model for plant biology.
378 Plant Cell Physiol **49**: 1084–1091

379 **Ishizaki K, Nishihama R, Ueda M, Inoue K, Ishida S, Nishimura Y, Shikanai T, Kohchi T**
380 (2015) Development of gateway binary vector series with four different selection markers
381 for the liverwort marchantia polymorpha. PLoS One **10**: 1–13

382 **Koi S, Hisanaga T, Sato K, Shimamura M, Yamato KT, Ishizaki K, Kohchi T, Nakajima K**
383 (2016) An Evolutionarily Conserved Plant RKD Factor Controls Germ Cell Differentiation.
384 Curr Biol **26**: 1–7

385 **Komatsu A, Kodama K, Mizuno Y, Fujibayashi M, Naramoto S, Kyozuka J** (2023) Control
386 of vegetative reproduction in Marchantia polymorpha by the KAI2-ligand signaling
387 pathway. Curr Biol **33**: 1196-1210.e4

388 **Kosugi S, Ohashi Y** (1997) PCF1 and PCF2 specifically bind to cis elements in the rice
389 proliferating cell nuclear antigen gene. Plant Cell **9**: 1607–1619

390 **Koyama T, Sato F, Ohme-Takagi M** (2017) Roles of miR319 and TCP transcription factors in
391 leaf development. Plant Physiol **175**: 874–885

392 **Kubota A, Ishizaki K, Hosaka M, Kohchi T** (2013) Efficient Agrobacterium-mediated
393 transformation of the liverwort Marchantia polymorpha using regenerating thalli. Biosci
394 Biotechnol Biochem **77**: 167–172

395 **Lin P-CC, Lu C-WW, Shen B-NN, Lee G-ZZ, Bowman JL, Arteaga-Vazquez MA, Liu L-**
396 **YD, Hong S-FF, Lo C-FF, Su G-MM, et al** (2016a) Identification of miRNAs and their

397 targets in the liverwort Marchantia polymorpha by integrating RNA-Seq and degradome
398 analyses. Plant Cell Physiol **57**: 339–358
399 **Lin P, Lu C, Shen B, Lee G, Bowman JL, Arteaga-vazquez MA, Liu LD, Hong S, Lo C, Su**
400 **G, et al** (2016b) Identification of miRNAs and Their Targets in the Liverwort Marchantia
401 polymorpha by Integrating RNA-Seq and Degradome Analyses Special Focus Issue –
402 Regular Paper. **57**: 339–358
403 **Lin SS, Bowman JL** (2018) MicroRNAs in Marchantia polymorpha. New Phytol **220**: 409–416
404 **Martín-Trillo M, Cubas P** (2010) TCP genes: a family snapshot ten years later. Trends Plant
405 Sci **15**: 31–39
406 **Palatnik JF, Allen E, Wu X, Schommer C, Schwab R, Carrington JC, Weigel D** (2003)
407 Control of leaf morphogenesis by microRNAs. Nature **425**: 257–263
408 **Palatnik JF, Wollmann H, Schommer C, Schwab R, Boisbouvier J, Rodriguez R,**
409 **Warthmann N, Allen E, Dezulian T, Huson D, et al** (2007) Sequence and expression
410 differences underlie functional specialization of Arabidopsis microRNAs miR159 and
411 miR319. Dev Cell **13**: 115–25
412 **Pietrykowska H, Sierocka I, Zielezinski A, Alisha A, Carrasco-Sanchez JC, Jarmolowski A,**
413 **Karlowski WM, Szweykowska-Kulinska Z** (2022) Biogenesis, conservation, and function
414 of miRNA in liverworts. J Exp Bot **73**: 4528–4545
415 **Rhoades MW, Reinhart BJ, Lim LP, Burge CB, Bartel B, Bartel DP** (2002) Prediction of
416 plant microRNA targets. Cell **110**: 513–520
417 **Romani F, Sauret-Güeto S, Rebmann M, Annese D, Bonter I, Tomaselli M, Dierschke T,**
418 **Delmans M, Frangedakis E, Silvestri L, et al** (2024) The landscape of transcription factor

419 promoter activity during vegetative development in Marchantia. Plant Cell **36**: 2140–2159

420 **Rövekamp M, Bowman JL, Grossniklaus U** (2016) Marchantia MpRKD Regulates the
421 Gametophyte-Sporophyte Transition by Keeping Egg Cells Quiescent in the Absence of
422 Fertilization. Curr Biol **26**: 1782–1789

423 **Shimamura M** (2016) Marchantia polymorpha: Taxonomy, phylogeny and morphology of a
424 model system. Plant Cell Physiol **57**: 230–256

425 **Solly JE, Cunniffe NJ, Harrison CJ** (2017) Regional Growth Rate Differences Specified by
426 Apical Notch Activities Regulate Liverwort Thallus Shape. Curr Biol **27**: 16–26

427 **Sugano SS, Nishihama R, Shirakawa M, Takagi J, Matsuda Y, Ishida S, Shimada T, Hara-**
428 **Nishimura I, Osakabe K, Kohchi T** (2018) Efficient CRISPR/Cas9-based genome editing
429 and its application to conditional genetic analysis in Marchantia polymorpha. PLoS One **13**:
430 e0205117

431 **Sugano SS, Shirakawa M, Takagi J, Matsuda Y, Shimada T, Hara-Nishimura I, Kohchi T**
432 (2014) CRISPR/Cas9-mediated targeted mutagenesis in the liverwort Marchantia
433 polymorpha L. Plant Cell Physiol **55**: 475–481

434 **Tsuboyama K, Tadakuma H, Tomari Y** (2018a) Conformational Activation of Argonaute by
435 Distinct yet Coordinated Actions of the Hsp70 and Hsp90 Chaperone Systems. Mol Cell **70**:
436 722-729.e4

437 **Tsuboyama S, Kodama Y** (2018) Highly efficient G-AgarTrap-mediated transformation of the
438 Marchantia polymorpha model strains Tak-1 and Tak-2. Plant Biotechnol **35**: 399–403

439 **Tsuboyama S, Nonaka S, Ezura H, Kodama Y** (2018b) Improved G-AgarTrap: A highly
440 efficient transformation method for intact gemmalings of the liverwort Marchantia

441 polymorpha. Sci Rep **8**: 1–10

442 **Tsuzuki M, Futagami K, Shimamura M, Inoue C, Kunimoto K, Oogami T** (2019) An Early
443 Arising Role of the MicroRNA156 / 529- SPL Module in Reproductive Development
444 Revealed by the Liverwort Marchantia polymorpha Report An Early Arising Role of the
445 MicroRNA156 / 529- SPL Module in Reproductive Development Revealed by the
446 Liverwort. Curr Biol **29**: 1–8

447 **Tsuzuki M, Nishihama R, Ishizaki K, Kurihara Y, Matsui M, Bowman JLJL, Kohchi T,**
448 **Hamada T, Watanabe Y** (2016) Profiling and characterization of small RNAs in the
449 liverwort, Marchantia polymorpha, belonging to the first diverged land plants. Plant Cell
450 Physiol **57**: 359–372

451 **Yamaoka S, Inoue K, Araki T** (2021) Regulation of gametangia and gametangiophore initiation
452 in the liverwort Marchantia polymorpha. Plant Reprod. doi: 10.1007/s00497-021-00419-y

453 **Yasui Y, Tsukamoto S, Sugaya T, Nishihama R, Wang Q, Kato H, Yamato KT, Fukaki H,**
454 **Mimura T, Kubo H, et al** (2019) GEMMA CUP-ASSOCIATED MYB1, an Ortholog of
455 Axillary Meristem Regulators, Is Essential in Vegetative Reproduction in Marchantia
456 polymorpha. Curr Biol **29**: 3987-3995.e5

457

458 **Figure Legends**

459 Fig. 1 (A) Primary *MIR319a* or *b* RNAs are predicted to be transcribed from two
460 annotated loci in the *M. polymorpha* genome. (B) The wild-type (WT) *MIR319a* locus
461 sequence targeted by gRNA#1 is presented. Mutants #5 and #10 were analyzed further.
462 (C) The WT *MIR319b* locus sequence targeted by gRNA#3 or #4 is presented. Mutants

463 #11 and #15 from the gRNA#3-treated pool and #6 and #9 from the gRNA#4-treated pool
464 were analyzed further. In the superscript *ge-x*, *x* indicates the gRNA species used to create
465 the mutant. (D) Changes in the *MIR319a* and *b* genomic loci in the double knockout line
466 *miR319ab #10/15*. The *MIR319a* locus had a 5-bp deletion and the *MIR319b* locus had a
467 1-bp insertion, similar to *miR319a*$^{ge-1}$ #10 and *miR319b*$^{ge-3}$. For simplicity, we named the
468 line *miR319ab #10/15*.
469
470 Fig. 2 (A) Disruption of the Mp*MIR319a* and/or *b* loci decreased the number of gemma
471 cups. Five plants were analyzed and the mean number of gemma cups per thallus is
472 presented. Tukey–Kramer's honestly significant difference test was performed to analyze
473 the variance. Statistically significant differences are indicated by different letters (a, b, c;
474 $P < 0.05$). (B) Appearance of different thalli. Bar = 1 cm. WT: Tak-1 wild-type plant, #5:
475 *miR319a*$^{ge-1}$ #5, #10: *miR319a*$^{ge-1}$ #10, #11: *miR319b*$^{ge-3}$ #11, #15: *miR319b*$^{ge-3}$ #15, #6:
476 *miR319b*$^{ge-4}$ #6, #10/15: *miR319ab* #10/15.
477
478 Fig. 3 Disruption of the Mp*MIR319a* and/or *b* loci inhibited gemma formation. (A)
479 Number of gemmae formed in each gemma cup. *$P < 0.05$ (Tukey method). (B)
480 Appearance of a gemma cup. Bar = 1 cm. WT: Tak-1 wild-type plant, #5: *miR319a*$^{ge-1}$ #5,
481 #10: *miR319a*$^{ge-1}$ #10, #11: *miR319b*$^{ge-3}$ #11, #15: *miR319b*$^{ge-3}$ #15.
482
483 Fig. 4 Exon–intron structures of Mp*RKD* and Mp*R2R3-MYB21* genes in the wild-type
484 form (or sensitive form, with prefix g) and miR319-resistant form (with prefix m) of (A)

485 Mp*RKD* and (B) mMp*R2R3-MYB21* genes. Vertical bars indicate conventional base-
486 pairing, whereas double dots indicate G–U pairs. AUG and UGA are initiation and
487 termination codons, respectively, of open reading frames. 5′UTR and 3′UTR refer to
488 untranslated regions.
489
490 Fig. 5 Introduction of the miR319-resistant mMp*RKD* gene suppressed gemma cup
491 formation in wild-type thalli, but the introduction of gMp*RKD* and mMp*MYB21* genes
492 did not.
493
494 Fig. 6 Introduction of the wild-type *RKD* gene (gMp*RKD*) induced normal gametophyte
495 development in Tak-1 (A, B) and Tak-2 (G, H). Introduction of the miR319-resistant
496 mutant *RKD* gene (mMp*RKD*) into Tak-1 induced the production of antheridiophores
497 with stalked receptables with irregular asymmetrical shapes (C, D) and antheridiophores
498 with exposed antheridia (E, F). Introduction of mMp*RKD* into Tak-2 induced the
499 production of archegoniophores with short digits (I,J), but normal archegonia (K).
500
501
502

Primers used in this study

primers to construct guide RNA vectors for establishment of *miR319a* or *miR319b* mutants

PAM_MIR319a-174f-F	CTCGACAATCCGTCCTTGGACTGA
PAM_MIR319a-174f-R	AAACTCAGTCCAAGGACGGATTGT
PAM_MIR319b-161r-F	CTCGAGCTCCCTTCAGTCCAAGTC
PAM_MIR319b-161r-R	AAACGACTTGGACTGAAGGGAGCT
PAM-MIR319b-179f-F	CTCGTTGGCCCGACTTGGACTGAA
PAM-MIR319b-179f-R	AAACTTCAGTCCAAGTCGGGCCAA

primers to construct miR319 resistant form Mp*RKD*

IF-Hind-pRKD-F	ACGACGGCCAGTGCCAAGCTTGGACACCGGAGAGAAATCAA
Inf-gMpRKD-Sal-R	CGGGGATCCTCTAGAGTCGACACACAAAGTTTTATAACGCCGATGT
mRWP_RK-F	CTGAATCGCAATCGAGCGGAGTTTCAAATCAAATAGAAGC
mRWP_RK-R	TCCGCTCGATTGCGATTCAGTATGTCATGAGACCAGGGTT

primers to construct miR319 resistant form Mp*R2R3-MYB21*

mMYB33-F	AGAATTGCCAAGTTCTCAGTCTGCAGAGTCTGCTGACAGC
mMYB33-R	ACTGAGAACTTGGCAATTCTAATTTCAGGCTGGAATTCGG
Hind-pMpMYB21-3000-F	GTTAAGCTTcgtgcccttgacctcctcctc
Sal-pMpMYB21-R	GTTGTCGACccaggcaccccagactcttgaac
Bam-MpMYB33-R2	GTTGGATCCGGGATAGGTCAGCAGGTCAGTAGT
pMYB33-459F	TGCCTGCCATGGCATACATCCCATC

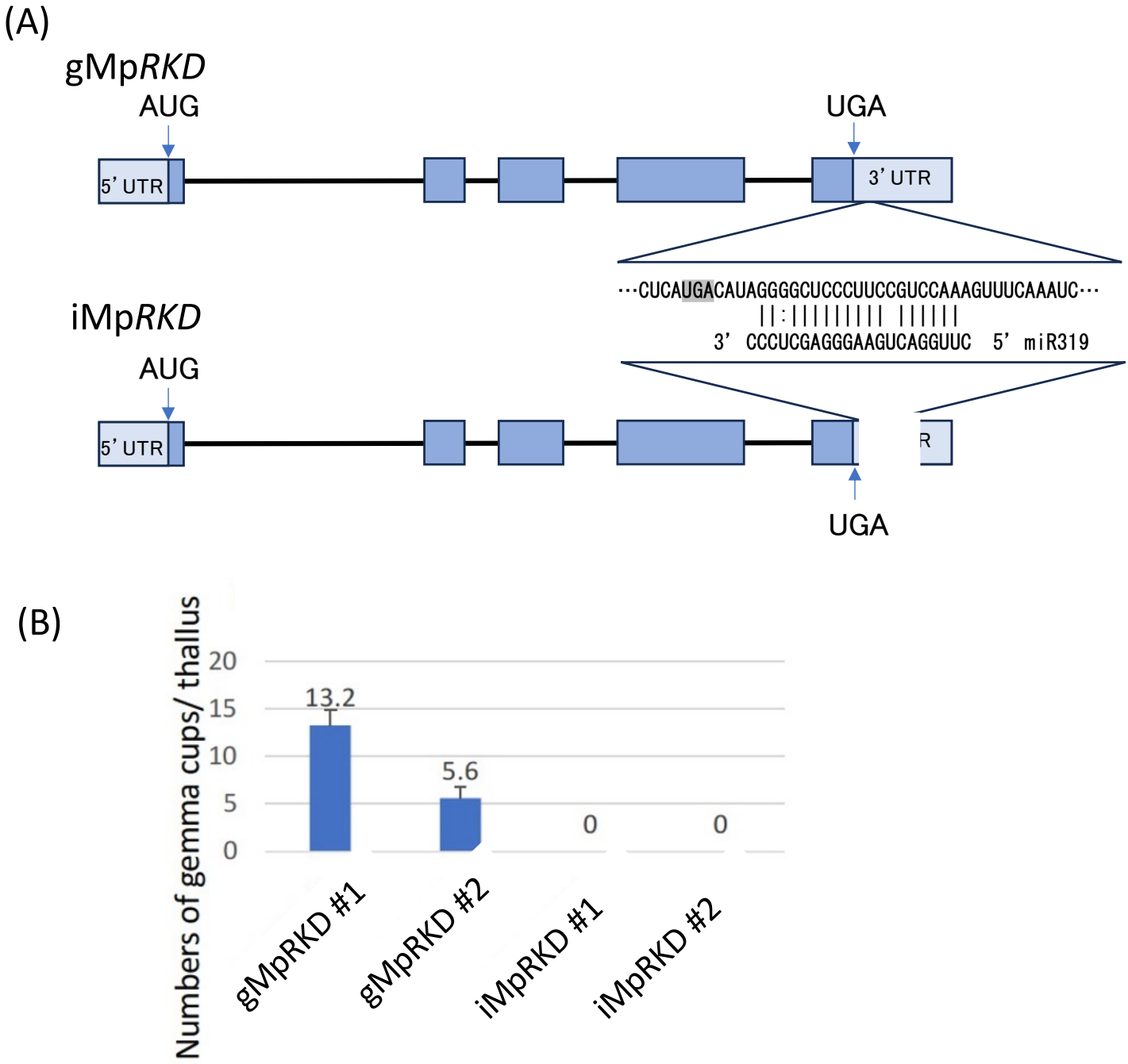

Fig.S1 Introduction of the miR319-insensitive iMp*RKD* gene suppressed gemma cup formation in thalli

(A) Construct of wild-type *RKD* (gMp*RKD*) and miR319 insensitive *RKD* (iMp*RKD*) genes. The sequence segment complementary to miR319 sequences located in 3' untranslated region (3' UTR) was deleted to obtain the iMp*RKD* gene. Each construct was placed under the direction of the promoter of Mp*RKD* and introduced into Tak-1 wild type plants to obtain respective transformants. (B) The numbers of gemma cups were counted per thallus for transformants.

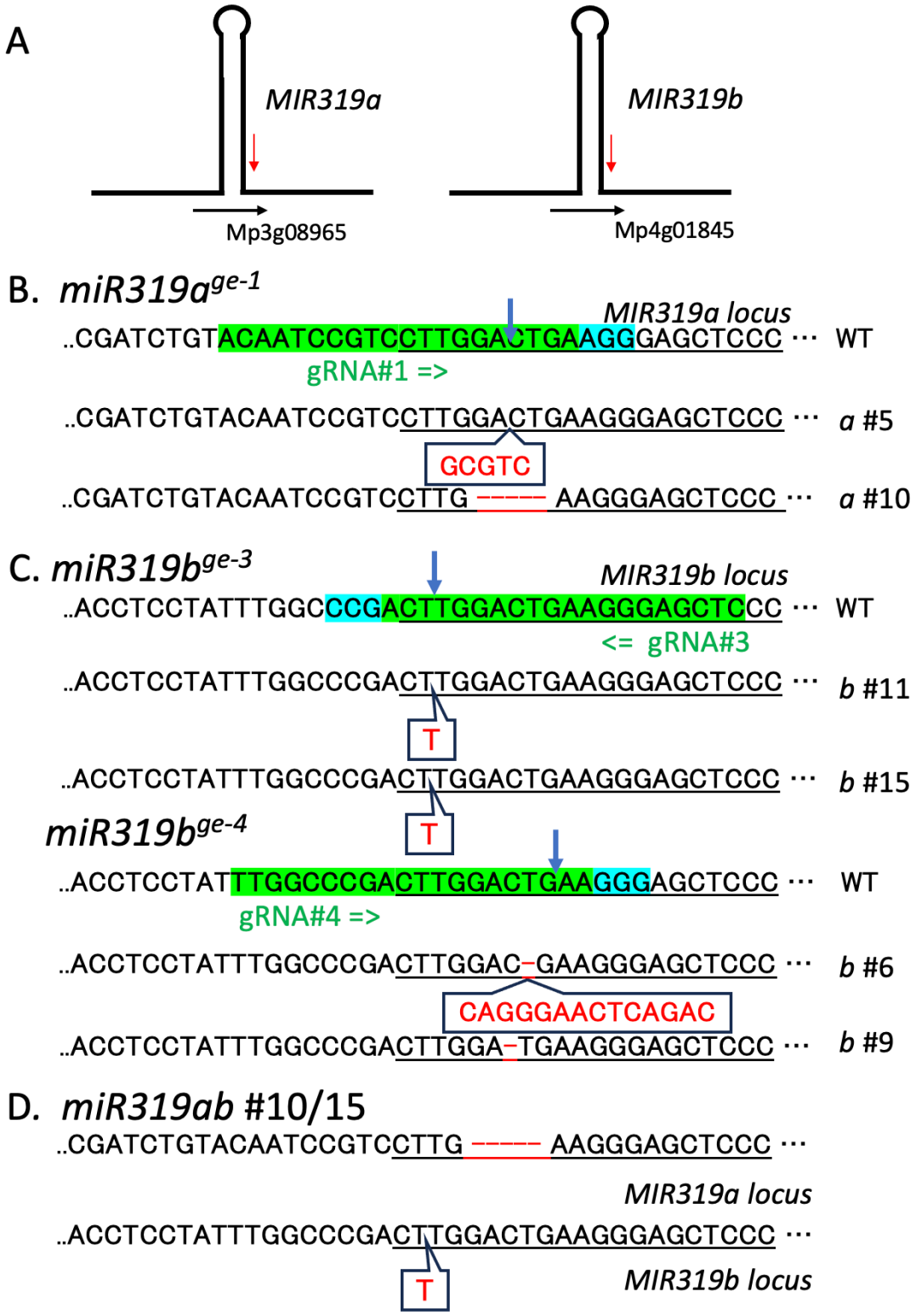

Fig. 1 (A) Primary *MIR319a* or *b* RNAs are predicted to be transcribed from two annotated loci in the *M. polymorpha* genome. (B) The wild-type (WT) *MIR319a* locus sequence targeted by gRNA#1 is presented. Mutants *a* #5 and *a* #10 were analyzed further. (C) The WT *MIR319b* locus sequence targeted by gRNA#3 or #4 is presented. Mutants *b* #11 and *b* #15 from the gRNA#3-treated pool and *b* #6 and *b* #9 from the gRNA#4-treated pool were analyzed further. In the superscript ge-x, x indicates the gRNA species used to create the mutant. (D) Changes in the *MIR319a* and *b* genomic loci in the double knockout line *miR319ab #10/15*. The *MIR319a* locus had a 5-bp deletion and the *MIR319b* locus had a 1-bp insertion, as did *miR319a*$^{ge-1}$ *a* #10 and *miR319b*$^{ge-3}$ *b* #15. For simplicity, we named the line *miR319ab* #10/15.

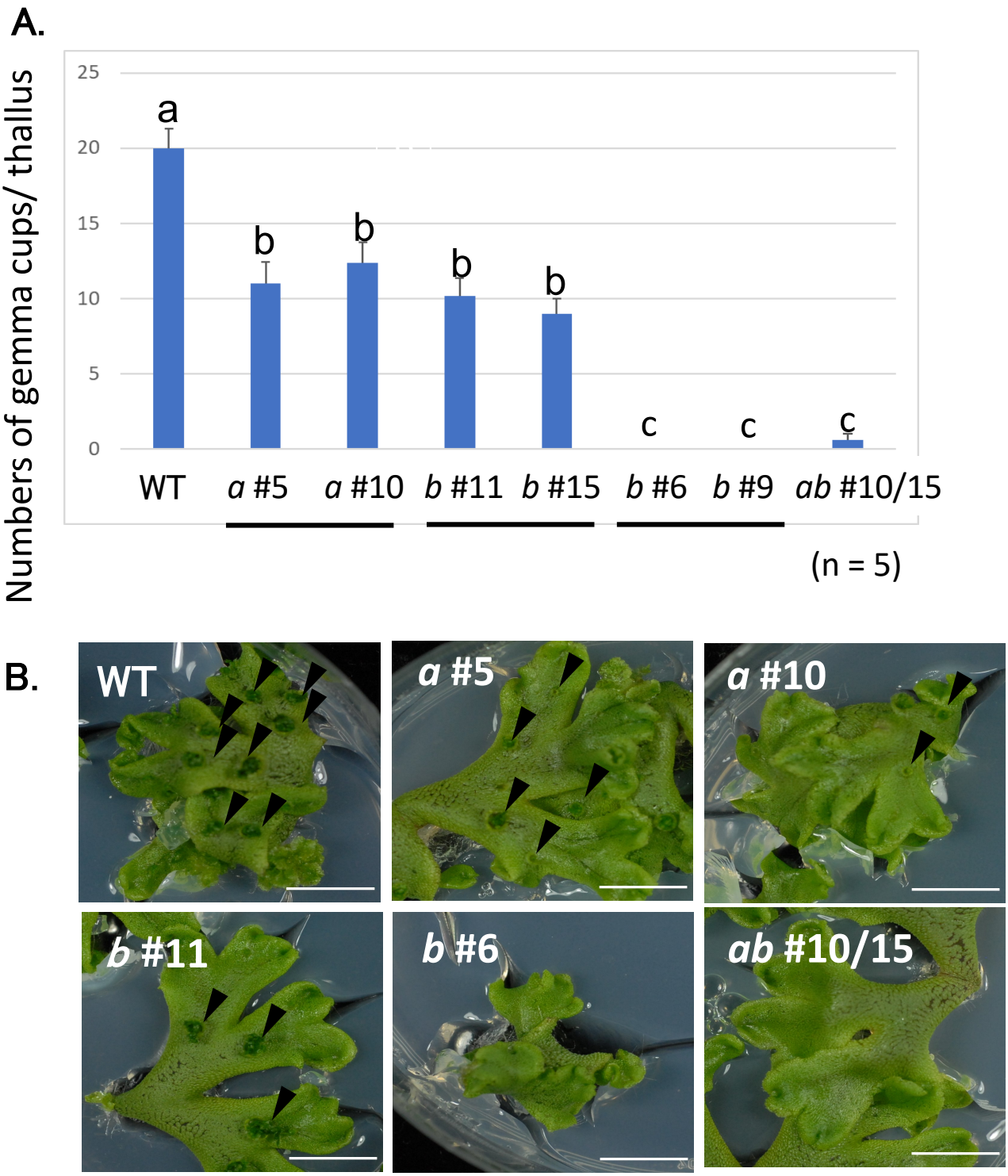

Fig. 2 (A) Disruption of the Mp*MIR319a* and/or *b* loci decreased the number of gemma cups. Five plants were analyzed and the mean number of gemma cups per thallus is presented. Tukey–Kramer's honestly significant difference test was performed to analyze the variance. Statistically significant differences are indicated by different letters (a, b, c; $P < 0.05$). (B) Appearance of different thalli. Bar = 1 cm. WT: Tak-1 wild-type plant, *a* #5: *miR319a*$^{ge\text{-}1}$ #5, *a* #10: *miR319a*$^{ge\text{-}1}$ #10, *b* #11: *miR319b*$^{ge\text{-}3}$ #11, *b* #15: *miR319b*$^{ge\text{-}3}$ #15, *b* #6: *miR319b*$^{ge\text{-}4}$ #6, *b* #9: *miR319b*$^{ge\text{-}4}$ #9, *ab* #10/15: miR319ab #10/15.

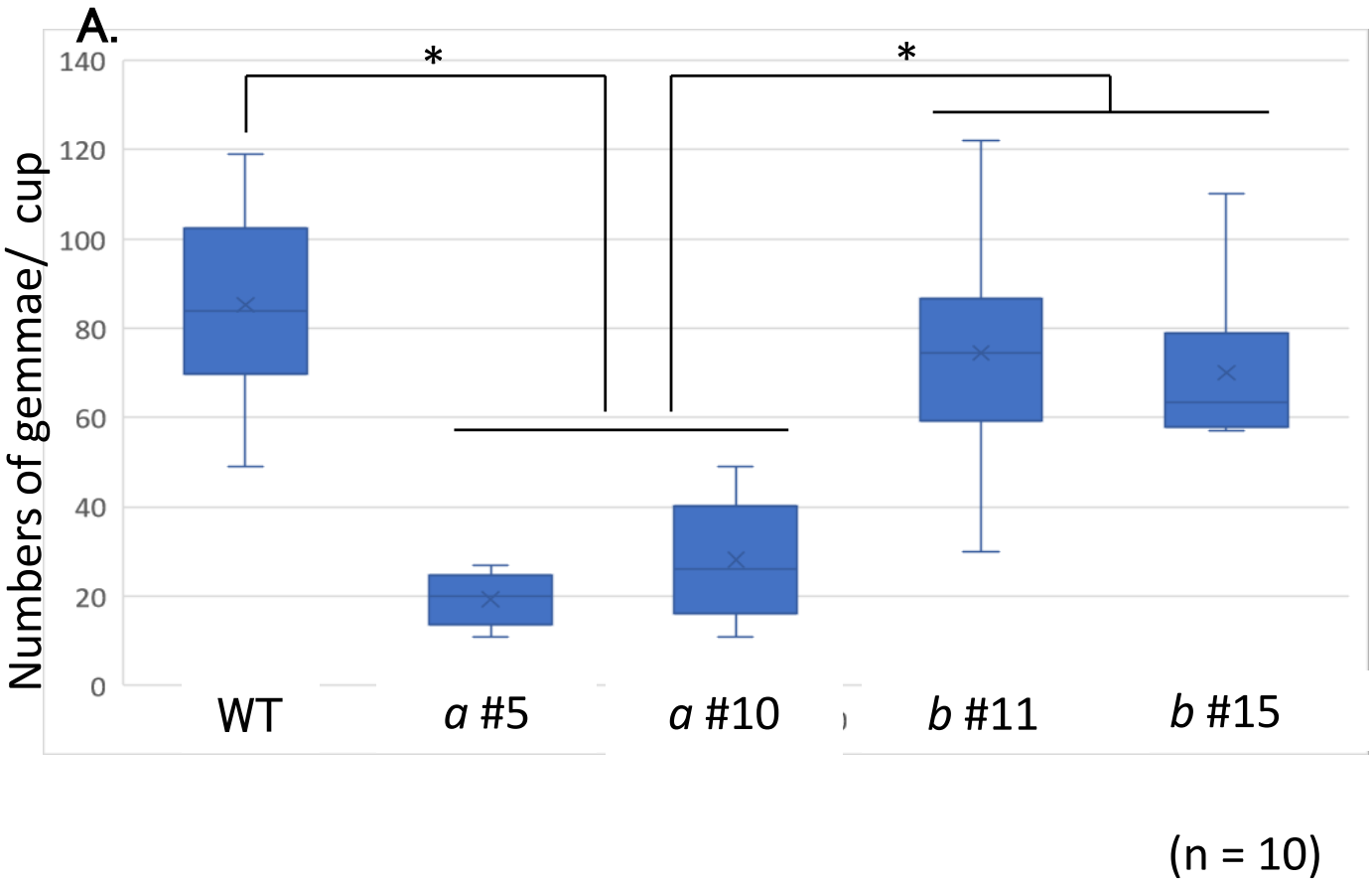

Fig. 3 Disruption of the Mp*MIR319a* and/or *b* loci inhibited gemma formation. (A) Number of gemmae formed in each gemma cup. *P < 0.05 (Tukey method). (B) Appearance of a gemma cup. Bar = 1 cm. WT: Tak-1 wild-type plant, *a* #5: *miR319a*$^{ge-1}$ #5, *a* #10*: miR319a*$^{ge-1}$ #10, *b #11*: *miR319b*$^{ge-3}$ #11, *b #115*: *miR319b*$^{ge-3}$ #15.

A. Mp*RKD*

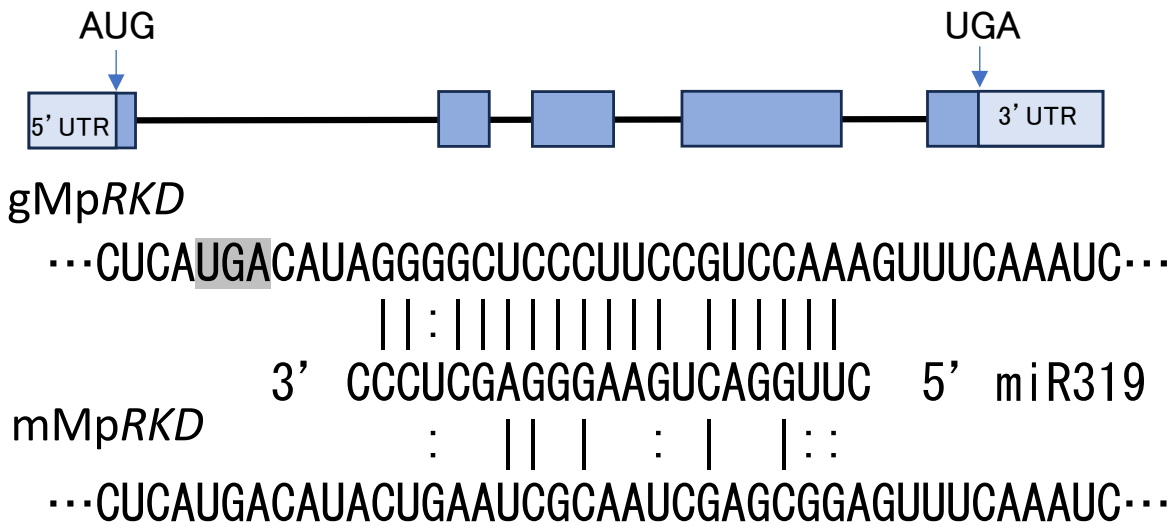

B. Mp*R2R3-MYB21*

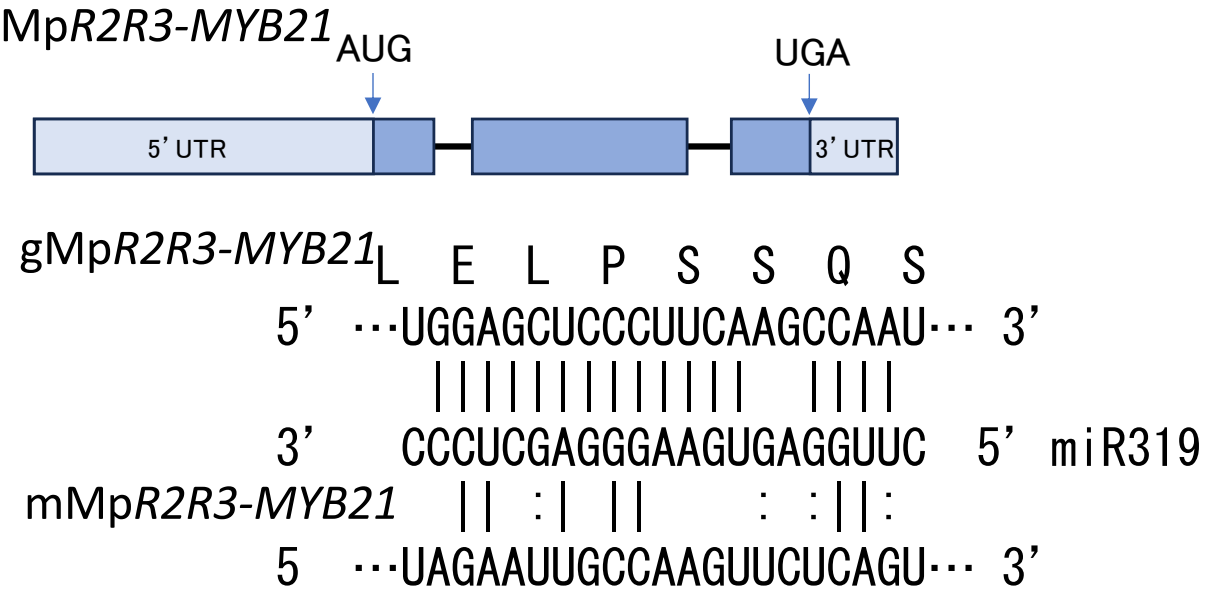

Fig. 4 Exon–intron structures of Mp*RKD* and Mp*R2R3-MYB21* genes in the wild-type form (or sensitive form, with prefix g) and miR319-resistant form (with prefix m) of (A) Mp*RKD* and (B) mMp*R2R3-MYB21* genes. Vertical bars indicate conventional base-pairing, whereas double dots indicate G–U pairs. AUG and UGA are initiation and termination codons, respectively, of open reading frames. 5′UTR and 3′UTR refer to untranslated regions.

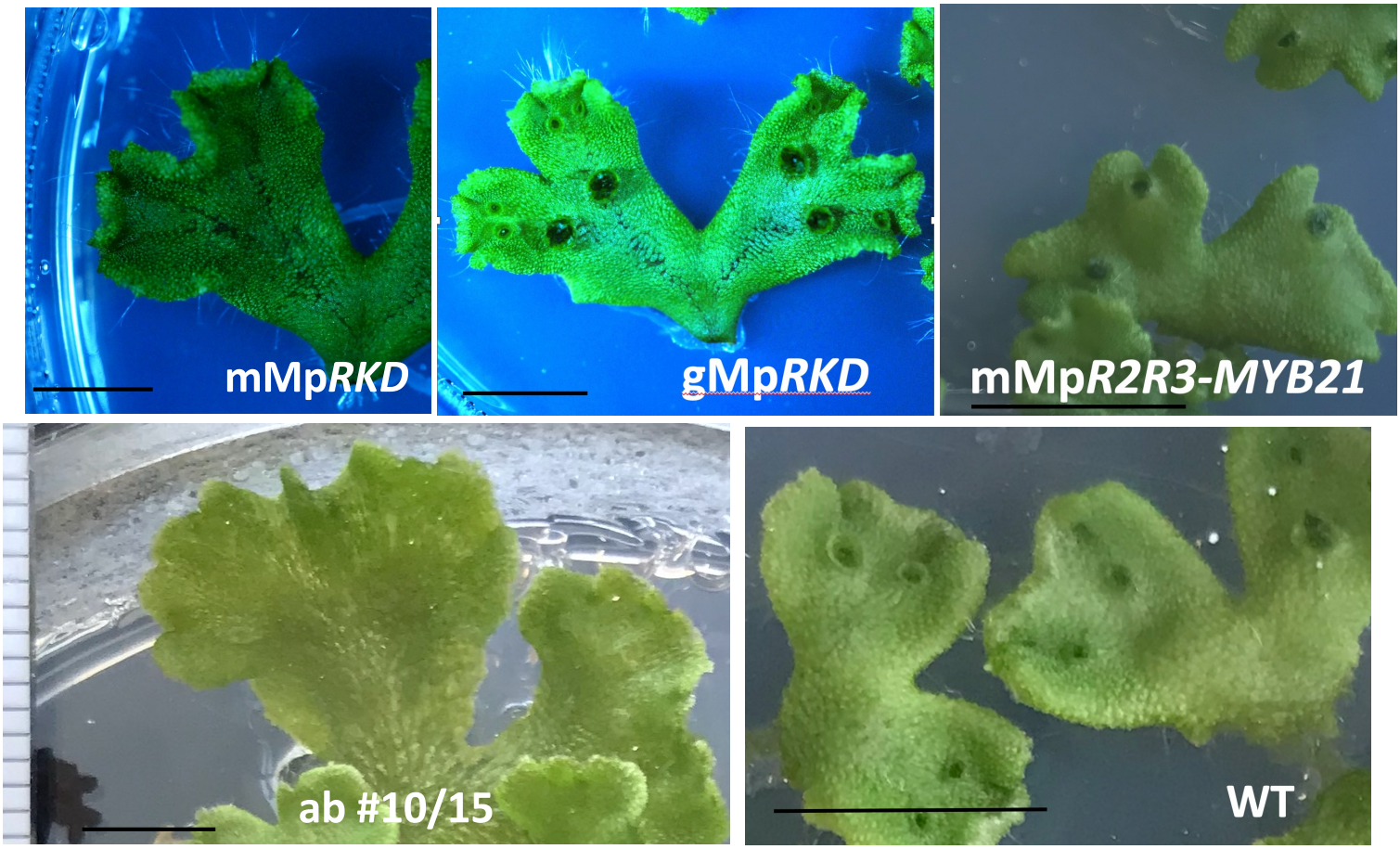

Fig. 5 Introduction of the miR319-resistant mMp*RKD* gene suppressed gemma cup formation in thalli, but the introduction of gMp*RKD* and mMp*R2R3MYB21* genes did not. Bar = 1 cm.

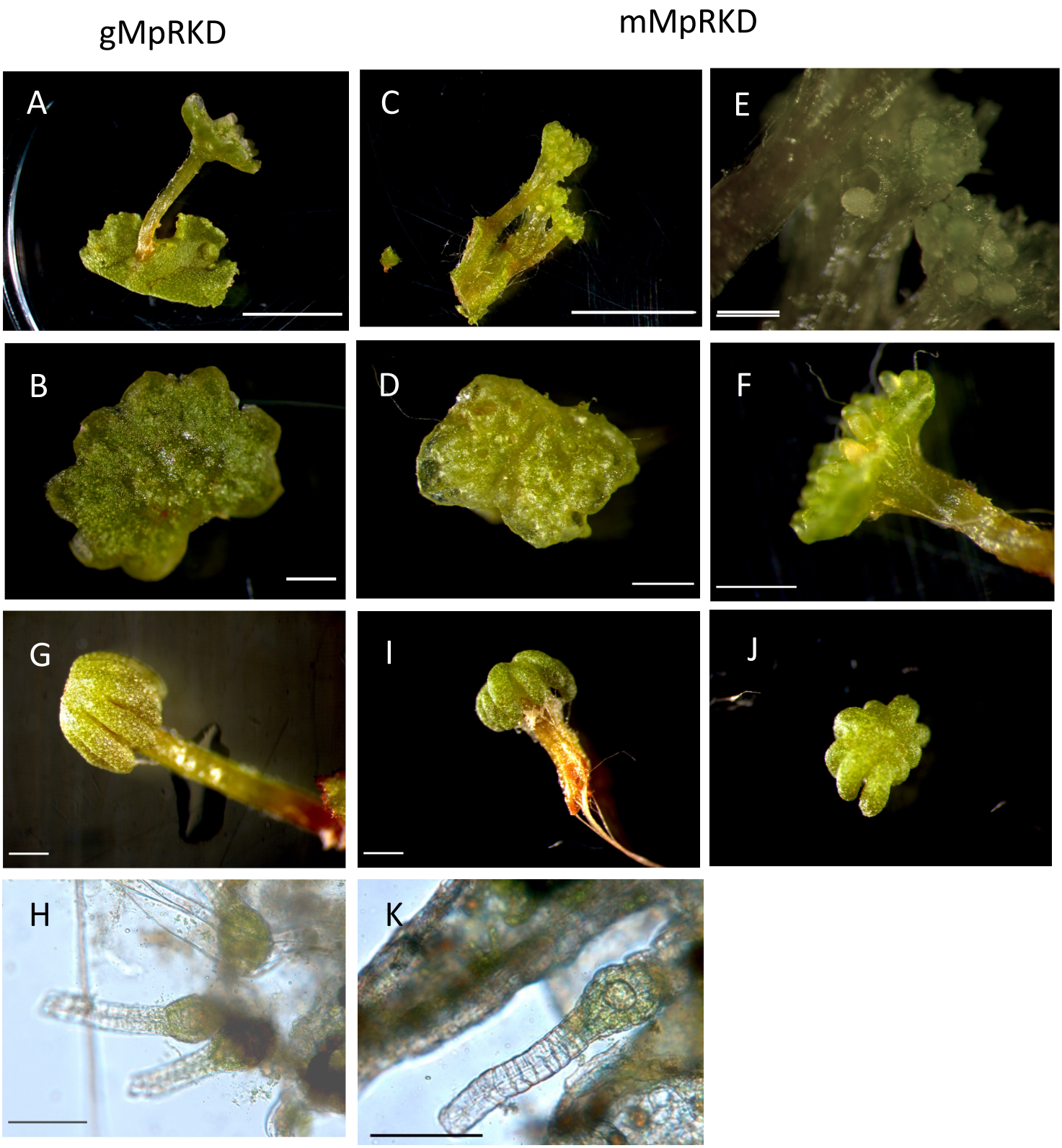

Fig. 6 Introduction of the wild-type *RKD* gene (gMp*RKD*) induced normal gametophyte development in Tak-1 (A, B) and Tak-2 (G, H). Introduction of the miR319-resistant mutant *RKD* gene (mMp*RKD*) into Tak-1 induced the production of antheridiophores with stalked receptables with irregular asymmetrical shapes (C, D) and antheridiophores with exposed antheridia (E, F). Introduction of mMp*RKD* into Tak-2 induced the production of archegoniophores with short digits (I, J), but normal archegonia (K).